

## RESEARCH ARTICLE



## OPEN ACCESS

Received: 09-11-2022

Accepted: 23-11-2022

Published: 31-12-2022

**Citation:** Syed ZF, Tamilarasan TR, Mohideen SR, Sanjana SM (2022) Optimization of Wear Parameters of Cryogenic and Heat-treated Al 6101 Closed-cell Foam using Taguchi Technique. Indian Journal of Science and Technology 15(48): 2765-2776. <https://doi.org/10.17485/IJST/v15i48.2158>

\* **Corresponding author.**

[tamilarasan.tr@crecident.education](mailto:tamilarasan.tr@crecident.education)

**Funding:** None

**Competing Interests:** None

**Copyright:** © 2022 Syed et al. This is an open access article distributed under the terms of the [Creative Commons Attribution License](https://creativecommons.org/licenses/by/4.0/), which permits unrestricted use, distribution, and reproduction in any medium, provided the original author and source are credited.

Published By Indian Society for Education and Environment ([iSee](https://www.indjst.org/))

**ISSN**

Print: 0974-6846

Electronic: 0974-5645

# Optimization of Wear Parameters of Cryogenic and Heat-treated Al 6101 Closed-cell Foam using Taguchi Technique

**Zeenath Fathima Syed<sup>1</sup>, T R Tamilarasan<sup>2\*</sup>, S Rasool Mohideen<sup>1</sup>, S M Sanjana<sup>3</sup>**

<sup>1</sup> Department of Mechanical Engineering, B.S.Abdur Rahman Crescent Institute of Science and Technology, Chennai, 600048, Tamil Nadu, India

<sup>2</sup> Department of Automobile Engineering, B.S.Abdur Rahman Crescent Institute of Science and Technology, Chennai, 600048, Tamil Nadu, India

<sup>3</sup> Department of Biomedical Engineering, Sri Ramakrishna Engineering College, Coimbatore, Tamil Nadu, India

## Abstract

**Objectives:** This study deals with the optimization of wear properties of Al 6101-alloy foam treated with different temperature zones such as Untreated (UT), Heat Treated (HT), Cryogenic Treated (CT), and Cryogenic Heat Treated (CHT), respectively. The results of this study concerning confirmation tests enable us to validate the proposed optimization findings for the coefficient of friction and specific wear. **Methods:** The Al 6101 foam samples used in this study are exposed to different heat and cryogenic treatments as well as wear tests using the pin-on-disk apparatus setup with the Taguchi optimization technique. The wear parameters are enhanced further using the Analysis of variance (ANOVA) technique, and this model is processed using the MINITAB software. The Al 6101 foam samples are evaluated using important wear testing parameters like Heat Zone, Load (N), Speed (rpm), and Sliding Distance (m), as well as the output parameters such as coefficient of friction and specific wear ( $\text{mm}^3/\text{Nm}$ ). **Findings:** The optimum combination of the coefficient of friction and specific wear, according to the graphic and analytical results of Taguchi's optimization, is with 40 N load, 400 rpm speed, and 1500 m distance for a cryogenic zone and 40 N load, 400 rpm speed, and 2000 m distance for a cryogenic heat zone, respectively. The interaction of sliding distance, load, and speed, which has probabilities of 17.42, 8.95, and 7.74, respectively, is followed by the coefficient of friction, which has a greater probability percentage of 48.01 for the heat zone. The ANOVA for the specific wear has a higher probability percentage of 48.82 for the load and is followed by the interaction of heat zone, sliding distance, and speed, which have probabilities of 37.59, 6.02, and 2.85, respectively. **Novelty:** Considering Al 6101 foam, which is mostly a non-ferrous material, this experiment once again confirmed that novel cryogenic treatment has a noteworthy improvement in coefficient of friction and specific



wear. Additionally, Taguchi's optimization and ANOVA analysis proved that the Al 6101 closed-cell foam specimen in the CHT zone exhibited optimal results when compared with other heat zones. The results confirmed that the CHT processing improves the wear resistance of the Al 6101 closed-cell foam effectively when examined with other different heat zones.

**Keywords:** Al 6101 ClosedCell Foam; Cryogenic Treatment; Taguchi Technique; Coefficient Of Friction; Specific Wear; Wear Graph; Surface Morphology; L16 Orthogonal Array; ANOVA

---

## 1 Introduction

Nowadays, Aluminium foam is developed into an unconventional novel material for structural applications. They possess remarkable mechanical, thermal, and electrical properties with low density<sup>(1)</sup>. They are highly suitable for lightweight structures and thermal insulation applications. Aluminium foams typically retain the valuable physical properties of base metals. The aluminium foam surface is porous by nature, due to this feature the thermal conductivity is significantly reduced however the coefficient of thermal expansion is comparable with the base metals<sup>(2)</sup>. Many patents were obtained in the cost-effective production methods of fabricating metallic foam. Al-alloy closed-cell foam is used as lightweight material and in damping processes in numerous engineering fields<sup>(3)</sup>. It has abundant potential in transportation sectors due to its energy-absorbing properties<sup>(4)</sup>. These categories of foams include applications in the aerospace, shipbuilding, construction, and blast industries<sup>(5)</sup>.

In the last four decades of the 20th century, cryogenic treatment for engineering materials has emerged as a relatively novel scientific approach to surface treatment. Materials such as ferrous and non-ferrous metal alloys, polymers, and ceramics are benefited from cryogenic treatment. It increases the microstructures and mechanical characteristics of the foam material considerably<sup>(6)</sup>. Cryogenic therapy has been recently updated as an effective approach for grain refinement, dimensional stability, and residual stress alleviation, as demonstrated by a variety of works of literature. Cryogenic treatment benefits wear resistance, thermal stability, homogenization, and enrichment of tool life and accordingly extends the service life of the components<sup>(7)</sup>.

Researchers explored how DCT influenced the wear properties of matrix and microstructures of self-lubricating iron composites<sup>(8)</sup>. The researchers revealed that deep cryogenic treatments improved tribological characteristics and stiffness. Paramjit Singh et al.<sup>(9)</sup> calculated the parametric adaptation of DCT to examine the wear and tribological output of the implant solid material UNS R56700, using Taguchi's optimization technique. The data suggested that the wear rate is influenced by factors such as soaking time, sliding speed, and contact pressure. Taguchi's S/N technique was utilized to examine the optimization of the wear response of Aluminium MMCs (356/B4Cp) by Udaya Prakash et al<sup>(10)</sup>. The wear test was executed using the L27 Orthogonal Array and it was utilized to establish the significance of the wear parameters. They showed that Taguchi's optimization methodology improved tribological properties. Researchers investigated the results of a deep cryogenic treatment in the wear testing parameters of an Al6101 alloy. Micro abrasive wear testing was performed on the specimen to understand more about the wear parameters. In addition, a microstructural analysis was performed. GP-zone identification is a factor in increased wear resistance in microstructural research. Divya Sadhana et al.<sup>(11)</sup> studied the Specific wear rate (SWR) of Aluminium LM25 alloy as the matrix material. An L27 orthogonal array was used to perform Taguchi's DOE. They employed an optimization method to demonstrate that the load influences the greatest statistical response on the input wear response rate. Cryogenic heat treatment (CHT) has an impact on account



of the tribological results of A356 Aluminium alloy reinforced with Silicon Carbide (SiC) by Sagar et al.<sup>(12)</sup>. According to their findings, both heat and cryogenic treatment improved tribological properties. Haidong Zhang et al.<sup>(13)</sup> calculated the results of a cryogenic treatment in the wear response properties, microstructures, and toughness of 42CrMo4 steel. Cryogenic treatment (CT) improves the toughness and the wear resistance property of 42CrMo steel, according to their research. Taguchi optimization and ANOVA techniques were utilized to study the wear of Al5083/CNT/Ni/MoB composite by Sajeeb Rahiman et al.<sup>(14)</sup>. They demonstrated that the layer creation between the sliding surfaces is one of the reasons for the composite sample's lower wear rate.

Limited research data on the mechanical characteristics of Aluminium alloy foam and the impacts of cryogenic treatments have come through authorized patents and previous publications. Cryogenic treatments' effect on the mechanical characteristics of Al 6101 closed-cell foam has recently acquired higher demand<sup>(15–17)</sup>. Despite this, no previous research has provided sufficient evidence to establish the wear resistance of Al6101 alloy foam treated with deep cryogenics. The main objective of this present study is to assess the wear and friction behavior of Al6101 alloy foam, as well as the optimization of tribological parameters of CHT zone Al6101 alloy foam, which is demonstrated using Taguchi's DoE optimization method.

## 2 Methodology

### 2.1 Specimen Preparation

Al6101 closed-cell foam is constructed with 98.5% pure Al6101 alloy. GFC Ltd., England, provided the material for this analysis. The Al6101 alloys offer better electrical conductivity and mechanical characteristics. The chemical composition of AL003860 includes Magnesium - 0.51%, Silicon - 0.43%, Zinc - 0.06%, Chromium - 0.03%, Manganese - 0.03%, Boron - 0.04%, Copper - 0.07% and Aluminium - 98.83%. The Al 6101 alloy foam holds specifications such as Porosity - 93%, Thickness - 30.0 mm, Mass density - 0.2 g/cm<sup>3</sup>, Purity - 98.50%, and 16 Pores/cm. Fig.1(a) shows the schematic diagram of the traditional Al 6101 closed-cell foam. For the wear test, an Al 6101 closed-cell foam specimen is prepared according to ASTM G99-05 specifications. Cutting the foam using traditional machining techniques is challenging. As a result, the specimen is made using a water jet machining cutter. The Dardi DWJ3020-BB Water Jet Cutter is utilized to prepare the Al 6101 foam specimen.

### 2.2 Cryogenic treatment

Before undergoing the cryogenic treatment, the prepared specimen is cleaned to get rid of any surface contaminants. The specimens are made to undergo heat, cryogenic, and cryogenic heat treatments. The specimen is heated to 350°C for 3 hours in a muffle furnace as part of the traditional heat treatment process, then it is gently cooled for 24 hours before being brought back to room temperature. The scientific cryogenic treatment process started with a 24-hour temperature change in the cryogenic chamber, starting from ambient to -195°C. Then, the chamber experienced a 24-hour cooling period before returning to normal temperature. After cryogenic treatment, the specimen is heated to 350°C for 3 hours, gradually cooled in the furnace for 24 hours, and then brought back to room temperature. The description of treatments are as follows: (1) HT - Three hours of heat treatment at 350°C, followed by 24 hours of cooling in the furnace and bringing it to room temperature, (2) CT - Undergone cryogenic therapy at -195°C for 24 hours, followed by cooling in the cryogenic chamber for additional 24 hours before returning to room temperature, (3) CHT - After the completion of cryogenic treatment, the tempering procedure is carried out at 350°C for 3 hours, then cooled for 24 hours before being brought down to room temperature, (4) UT - As received material.

### 2.3 Wear Testing mechanisms

To assess the materials for friction and wear resistance, various tribometers are utilized. One of the most often utilized wear testing and analysis methodologies is the pin-on-disc test device. The method's appeal stems from its comparative simplicity of implementation and the vast number of tribological interactions that could be characterized using this single pin-on-disk motion apparatus. This is utilized for numerous motions such as unidirectional, fretting, and other sophisticated motion patterns for tribological analysis. The tests are conducted as per ASTM G99-05.

The wear experiment is carried out utilizing the computer-based data collection pin-on-disc wear testing apparatus named Ducom Wear Tester-TR-201 CL wear and friction monitor. The wear test is done under dry sliding conditions at a room temperature of 25°C. Before testing, the worn track and closed cell Al 6101 Aluminium foam specimens are cleaned completely with acetone. The pins are created from a sample of Al 6101 closed-cell aluminium foam, measuring 15 mm in length and 12 mm in diameter. The foam sample is then fixed in the tribometer's pin holder to make it ready for wear testing. Four different sliding speeds are used in the wear testing on AISI D2 high carbon-high chromium steel discs with a hardness of 65 HRC. Four different sliding speeds used in the wear machine are at 400 rpm (1.6740 m/s), 500 rpm (2.0933 m/s), 600 rpm (2.512 m/s), and



700 rpm (2.930 m/s) respectively. The mass loss induced by the wear response is estimated with an electronic balance with an accuracy of 0.01 mg. The track's diameter is fixed to 80 mm, and the weight, sliding speed, and sliding distance are all fixed to the exact values. The arm is bound to keep contact with the disc till the contact surface wears away due to the force of the load. A signal is generated by the arm movement, which is utilized to calculate the maximum wear.

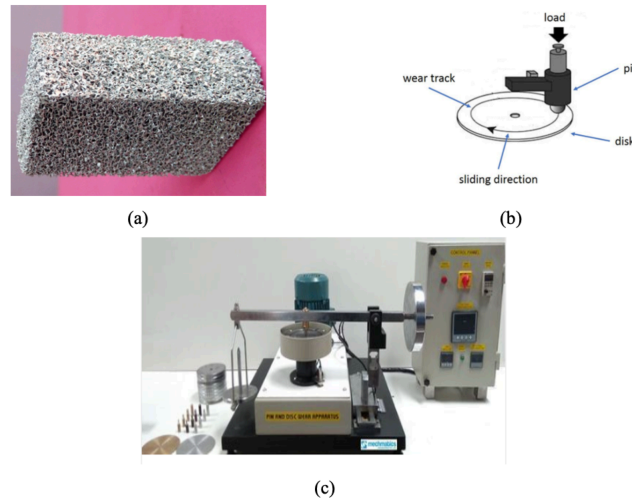


**Fig 1.** Articulation of (a) Al 6101 Closed-cell Foam, (b) Pin-on-Disc Apparatus, and (c) Schematic setup

The schematic illustration of the pin-on-disc apparatus and schematic setup is shown in Figure 1 (b) and Figure 1 (c). The stationary pin pushes beside the rotating disc when the proper weight is provided. Although the pin can be any shape, spherical (ball or lens) and cylindrical versions are the most common for theoretical analysis due to their ease of alignment. During the test, the temperature, wear, and friction force are all constantly monitored. Wear is determined by the amount of volume lost per test. The wear volume is determined using mass loss and density of the material. The speed and radius at which the pin is held from the disk's center are utilized to determine the wear velocity and sliding distance. The mathematical expressions below are adopted to calculate the specific wear and coefficient of friction.

(1) Sliding Velocity =  $\pi DN / 60$  (m/s); (2) Wear Volume =  $\Delta V$  (Volume loss in  $\text{mm}^3$ ); (3) Specific wear rate =  $\Delta V / (L X d)$ ; (4) Co-efficient Of Friction (COF) =  $FF / (L)$ , where  $D$  represents the track diameter (mm),  $N$  signifies the speed (rpm),  $L$  is the load in (N),  $d$  corresponds to the sliding velocity (m), and  $FF$  is the frictional force.

## 2.4 Tribological Analysis by Taguchi's Approach

Genichi Taguchi invented the Taguchi technique, which is a type of Design of Experiments (DoE) that is used to explore several factors that impact the mean and variance of a response parameter. The orthogonal arrays integrate the use of the influencing components of the process with the levels at which they have to be altered. With the least amount of trial time and expense, it enables the collection of vital data to determine the factors that have the most impact on product quality.

Depending on the number of parameters and levels, the appropriate orthogonal array is selected. The wear rate of an Al 6101 Foam specimen during dry sliding motion is investigated in this study. Taguchi's experiment incorporated four variables, each with four levels of variation as Applied Heat Zone, Load, Speed, and Sliding Distance. Tables 1 and 2 list the parameters of the experiment, along with their appropriate levels.

An orthogonal array's degree of freedom must be more than or equal to the total wear factors. Therefore, L16 Orthogonal array with 16 rows and 4 columns is selected, and 16 trials are carried out using the Taguchi model's experimental run order. The model includes responses such as coefficient of friction (COF) and specific wear (SW). The Heat Zone is represented by the first column of an orthogonal array, whereas the Load, Speed, and Sliding Distance are represented by the second, third, and fourth columns, respectively. The COF and SW are the response factors of the model.



**Table 1.** Wear Testing parameters and their levels

Symbols	Parameters	Levels			
		1	2	3	4
H	Heat Zone	UT	HT	CT	CHT
L	Load (N)	10	20	30	40
S	Speed (rpm)	400	500	600	700
SD	Sliding Distance (m)	1000	1500	2000	2500

**Table 2.** Wear Testing parameters and their outputs (Standard  $L_{16}(4)^4$  Orthogonal Array)

Experiment Trials	Heat Zone	Load (N)	Speed (rpm)	Sliding Distance (m)	CoF	Specific Wear $10^{-8} \text{ mm}^3 / \text{Nm}$
1	UT	10	400	1000	0.64592	7.5
2	UT	20	500	1500	0.73857	6.43
3	UT	30	600	2000	0.66249	3.05
4	UT	40	700	2500	0.56127	3.3
5	HT	10	500	2000	0.71377	6.6
6	HT	20	400	2500	0.8115	3.26
7	HT	30	700	1000	0.73781	3.93
8	HT	40	600	1500	0.75168	1.88
9	CT	10	600	2500	0.72023	5.08
10	CT	20	700	2000	0.6712	2.7
11	CT	30	400	1500	0.85805	2.6
12	CT	40	500	1000	0.89792	2.95
13	CHT	10	700	1500	0.5824	4.06
14	CHT	20	600	1000	0.53126	2.45
15	CHT	30	500	2500	0.20191	1.17
16	CHT	40	400	2000	0.58879	1.06

### 3 Results and Discussion

#### 3.1 Influence of cryogenic treatment on wear response and friction behavior

Figure 2 a-d shows the impact of deep cryogenic treatment on Al 6101 closed-cell Aluminium foam corresponding to the wear metrics.

As shown in Figure 2 a-d, the COF is high at the beginning of the test and gradually decreases throughout the test duration. The running-in effect is a common occurrence in friction measurements. The surface topography varies during the running-in process, and chemical reactions take place until the system stabilizes. The test comes to an end after a predetermined number of cycles, and data processing methods usually incorporate surface topography analysis to calculate the rate of wear and friction coefficient. The coefficient of friction lies between 0-0.2 for the CHT zone while in all the other zone specimens it starts from 0.2 to 0.9. CHT zones have a lower coefficient of friction than all other zones, according to the wear graph in Figs.2a-2d. The results for the CHT zones are considerably different when compared with the coefficient of friction values in the UT, HT, and CT zones.

##### 3.1.1 The outcome of Applied Load

In Al 6101 closed-cell Aluminium alloy foam with different heat treatments, Figure 3 (a) shows the effect of applied load on specific wear rate and average friction coefficient. In heat treatment, the foam sample's specific wear rate and average friction coefficient both dropped considerably. The average friction coefficient for sliding on a steel disc changes as the load increases. All specimens in all heat-treated zones had an identical pattern. This might be owing to the specimen's unexpected load-bearing capabilities after being thermally and cryogenically processed. As the load increases, the specific wear drops. This phenomenon is apparent from the wear graph, CHT specimens have a much-reduced friction coefficient and specific wear (Figure 4 (i)).



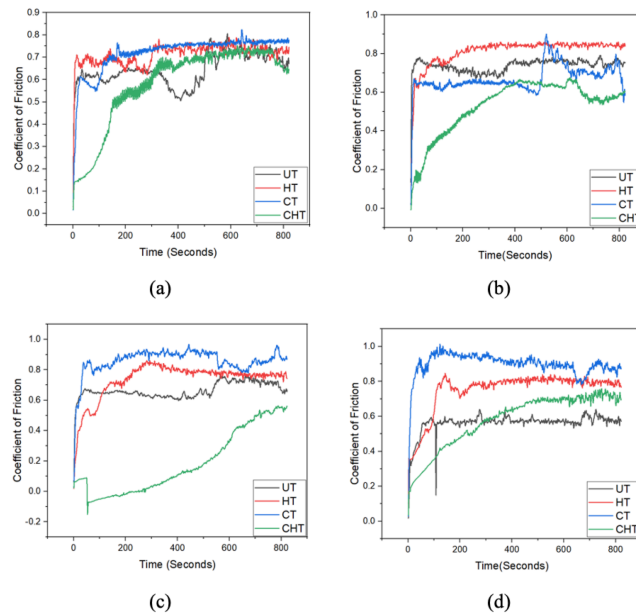


**Fig 2.** (a) Wear graph of specimens (UT, HT, CT, CHT) illustrating the circumstances for a load-10 N, speed- 400 r/min, sliding distance -1000 m, (b) Wear graph of specimens (UT, HT, CT, CHT) demonstrating the circumstances for a load-20 N, speed- 500 r/min, sliding distance -1500 m, (c) wear graph of specimens (UT, HT, CT, CHT) depicting the circumstances for a load-30 N, speed- 600 r/min, sliding distance-2000 m, and (d) wear graph of specimens (UT, HT, CT, CHT) showing the circumstances for a load-40 N, speed- 700 r/min, sliding distance -2000 m

The cryogenic heat-treated specimens exhibited lower coefficients of friction and specific wear rates than the untreated and heat-treated specimens in the experimental trials.

### 3.1.2 The outcome of Sliding Speed

Figure 3 (b) shows that the average coefficient of friction and specific wear is affected by sliding speed. The rate of wear decreases as the sliding speed increases from 400 to 700 rpm. As speed increases, the average coefficient of friction in the UT zone decreases. In the (HT) heat-treated zone, similar observations are made. The CT and CHT zones have different outcomes. In the CT and CHT zones, the average coefficient of friction decreases. When compared with UT and HT zones, the wear rate in the CT and CHT zones is also lower. Cryogenic-treated specimens exhibit a lower coefficient of friction and specific wear rate, as shown in the wear graph (Figure 2 a-d). Compared to the experimental trials, the cryogenic heat-treated specimens had reduced coefficients of friction and specific wear rates.

### 3.1.3 The outcome of Sliding Distance

Figure 3 (c) shows the effect of sliding distance on the specific wear rate and the average coefficient of friction of foam specimens. The wear rate increases from 1000 to 2500 meters. From 1000 to 2000 meters, the average coefficient of friction increases and then decreases till it reaches 2500 meters. Cryogenic heat-treated specimens also possess a much lower specific wear rate. In comparison to the trials of investigations, the cryogenic heat-treated specimens exhibited reduced coefficients of friction and specific wear.

The surface morphology of the Al 6101 foam specimen is presented in Figure 4 . Wear surface studies, particularly in the subsurface regions, are needed to understand the primary causes of friction and material loss rates during wear. Wear starts in the subsurface sections of interacting sliding surfaces and progresses to the top surface. Plastic deformation occurs in metallic alloys as a result of sliding contact, which usually leads to recrystallization and crystallographic roughness. Small fractures in the subsurface areas of brittle materials are the most common source of wear deterioration. The elemental and chemical contents of worn surfaces are examined using X-ray and electron spectroscopy, as well as SEM examination. All heat and cryogenic treated zones had small particle, abrasive, and adhesive wear mechanisms visible in the foam specimens. Gradual and minor wear is perceived on the specimen's surface as a result of the pressure concentration. Significant fragmentation and abrasive wear have



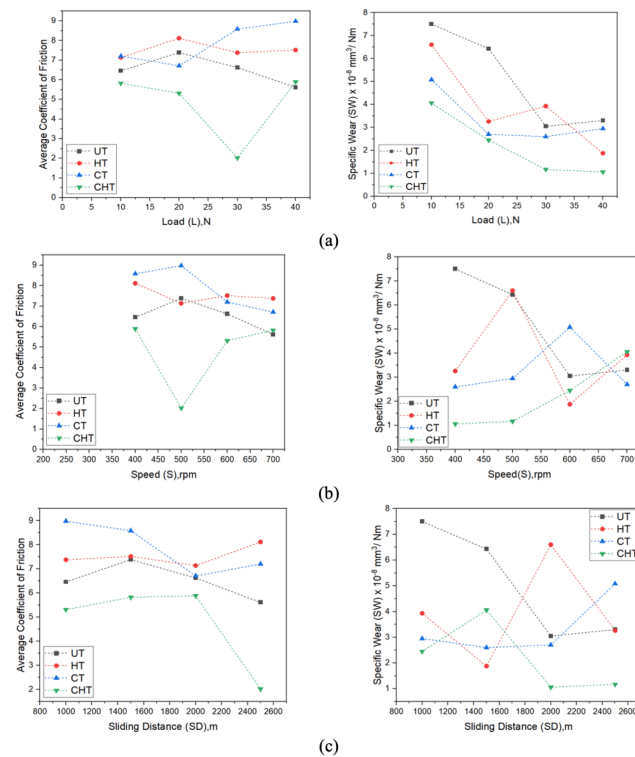


**Fig 3.** Wear Graph: untreated zone (UT), Heat treated zone (HT), Cryogenic treated Zone (CT), and Cryogenic Heat-Treated Zone (CHT) (a) Applied Load, (b) Sliding Speed, and (c) Sliding Distance

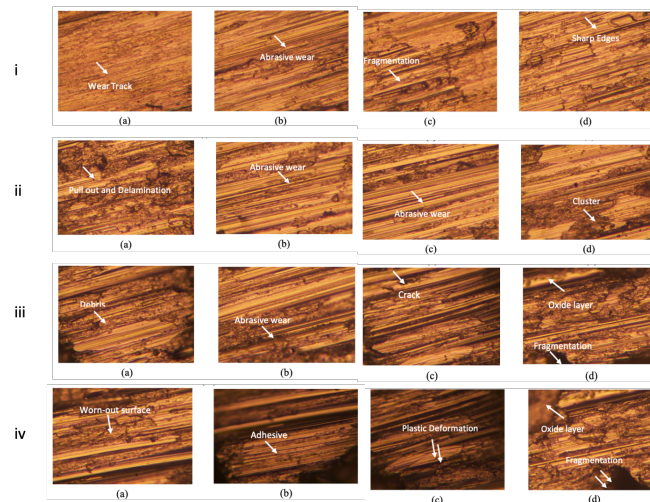


**Fig 4.** (i) Surface morphology of Al 6101 Specimens in the Untreated Zone (UT), (ii) Surface morphology of Al 6101 Specimens in the Heat Zone (HT), (iii) Surface morphology of Al 6101 Specimens in the Cryogenic Zone (CT), (iv) Surface morphology of Al 6101 Specimens in the CH Zone (CHT) - (a) For the parameters load 10 N, speed 400 r/min, and Sliding Distance 1000 m, (b) For the parameters load 20 N, speed 500 r/min, and Sliding Distance 1500 m, (c) For the parameters load 30 N, speed 600 r/min, and Sliding Distance 2000 m, and (d) For the parameters load 40 N, speed 700 r/min, and Sliding Distance 2500 m



occurred in the UT Foam samples (Figure 4 (i)). As a result of abrasive wear, sharp edges are also produced on the surface. Pull-out and delamination are seen in the HT zone specimen. Abrasive wear and cluster formation is observed in this area (Figure 4 (ii)). Aluminium is essentially a ductile material that, when cryogenically treated, transforms from ductile to brittle. Because of this brittle transition property, cracks appear in the cryogenically treated foam material. The CT zone foam samples can also display fragmentation and abrasive wear events. The formation of an oxide layer (Figure 4 (ii)) is one of the main reasons to reduce the wear rate because the oxide layer keeps the hard counter surface from coming into direct contact with it. Another factor that affects wear is surface roughness. Adhesion is aided by it. On the CHT zone specimen, adhesion wear phenomena are perceived (Figure 4 (iv)). At low and intermediate speeds, adhesive and abrasive wears predominate, while melting wear is localized at high speeds. Figure 4 (iv) shows the evaporation of a worn-out surface. The specimen's surface also displayed signs of plastic deformation and disintegration. It is likewise possible to see the formation of an oxide layer at a faster sliding speed. The oxide layer serves as a lubricant to the sliding surfaces, reducing wear.

### 3.2 Signal-to-Noise ratio analysis

The coefficient of friction and specific wear in  $\text{mm}^3/\text{Nm}$  are the two output response parameters of a pin-on-disc Tribometer with four customizable input variables being used in the experiments. The applied load-to-frictional force ratio is used to calculate the coefficient of friction, and the volume loss to load and sliding distance product to calculate the specific wear. The logarithmic Taguchi Signal-to-Noise (S/N) ratios serve as an objective function for the optimization of wear parameters. The significance of the controllable element is examined using the S/N ratio approach. Wear performance should increase if COF and SW are all smaller. As a result, the S/N ratio is determined for COF and SW in this study using the smaller-the-better methodology,

where  $y_1, y_2, \dots, y_n$  represents the experimental results or observations and the variable  $n$  represents the number of experiments.

The experimental results, including coefficient of friction and specific wear, from dry sliding wear tests, and Taguchi's method is used to optimize the wear parameters. Since the objective of this study is intended to attain the lowest possible coefficient of friction and specific wear, the lower-the-better quality characteristic is used. The S/N ratio response table is used to discover the optimal input parameter combination for the desired output characteristic. Expt. 15 has the best combination of CHT heat zone, 30 N load, 500 rpm speed, and 2500 m sliding distance for a COF of 0.20191 and an S/N ratio of 13.89702 db. Expt. 16 has the best combination of CHT heat zone, 40 N load, 400 rpm speed, and 2000 m sliding distance for an SW of 1.06 and S/N ratio of -0.50612 db.

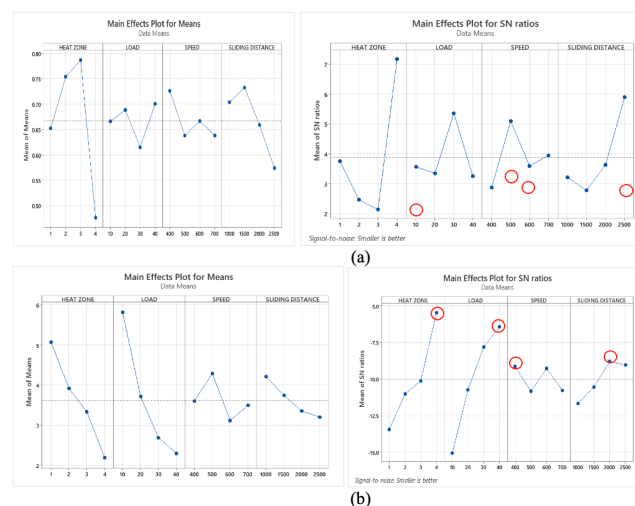


Fig 5. Main effect plot for (a) Coefficient of friction, and (b) Specific wear

Figure 5 shows the results of all the analyses as an output. The ideal conditions to obtain the lowest coefficient of friction (Figure 5 (a)) and the lowest specific wear (Figure 5 (b)) are presented. The best parameters to obtain the least amount of friction are in the CT Zone with a load of 40 N, a speed of 400 rpm, and a sliding distance of 1500 m for a coefficient of friction of 0.19891 with a corresponding S/N ratio of 13.6905 dB, and the best parameters to attain the least amount of specific wear are in the CHT



Zone with a load of 40 N, a speed of 400 rpm, and a sliding distance of 2000 m for specific  $0.9 \times 10^{-8}$  ( $\text{mm}^3/\text{Nm}$ ) with the S/N ratio of 0.0429 dB.

### 3.3 Mathematical modeling

In this study, linear regression analysis in Minitab 19 is used to build a predictive empirical model for the dependent variables COF and SW are a function of heat zone, load, speed, and sliding distance. All reactions have not been transformed. The regression model for Friction coefficient and Specific Wear rate is created using the parameters Heat Zone (H), Load (L), Sliding distance (D), and Sliding speed (S). The predictive equation obtained from the regression analysis for the coefficient of friction and specific wear is shown in Equations (2), and (3). The value of  $R^2$  is used to calculate the fitness of the created models. The values of the coefficient of determination range from 0 to 1. If the value is near one, it recommends the dependent and independent variables are well-matched. The constructed regression models for COF with  $R^2$  values are 82.13%, while the  $R^2$  values for (SW) are 95.30 %. The coefficients in the proposed model are checked for significance using the residual plot. If the residual plot is a straight line, the residual error is normally distributed in the model, and the coefficients are significant.

### 3.4 Regression Equation

$$\text{Coefficient of friction (COF)} = 1.075 - 0.0495H + 0.00030L - 0.000235S - 0.000092S \quad (2)$$

$$\text{Specific Wear (SW)} = 10.84 - 0.924H - 0.1156L - 0.00150S - 0.000681SD(3) \quad (3)$$

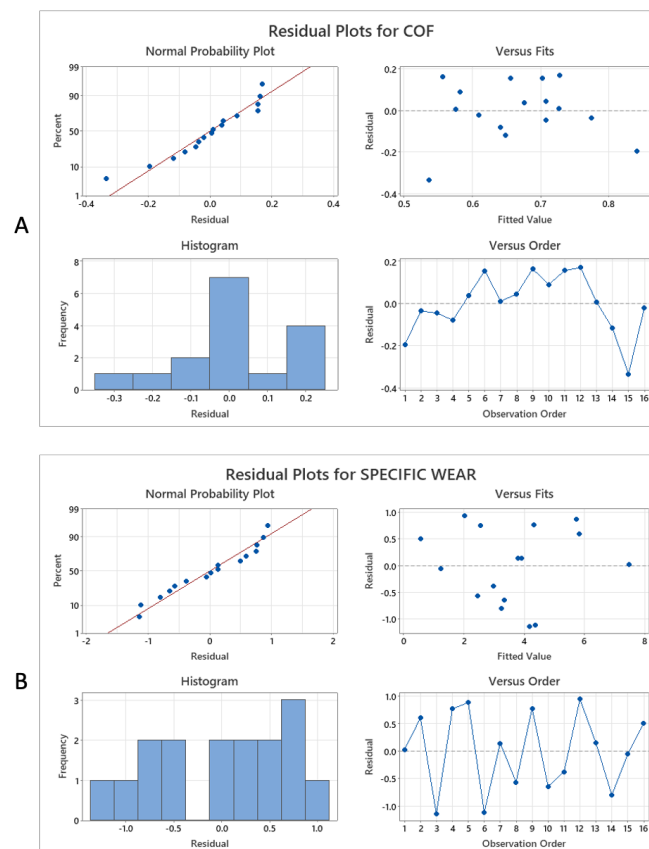


Fig 6. Residual plot: (a) coefficient of friction, and (b) Specific Wear

The residuals are observed to be close to the straight line, indicating that the built models are legitimate (Figure 6). The testing results are obtained using the L16 orthogonal experimental design. According to the confirmation findings, the models'



projected outcomes are in good agreement with the given range of parameters.

### 3.5 ANOVA for Coefficient of friction (COF) and Specific wear (SW)

The main characteristics of the coefficient of friction and specific wear are revealed by the analysis of variance for the given response. The combination of sliding distance, load, and speed follows the coefficient of friction, which has a greater probability percentage of 48.01 for the Heat Zone, with probabilities of 17.42, 8.95, and 7.74, respectively.

**Table 3.** ANOVA of Coefficient of friction and Specific wear

ANOVA of Coefficient of friction				
Source	Degrees of Freedom (DOF)	Sum of squares (SS)	Mean Square (MS)	Percentage Contribution
H	3	63.45	21.15	48.01
L	3	11.83	3.944	8.95
S	3	10.23	3.41	7.74
SD	3	23.02	7.675	17.42
Total	15	132.16		100
ANOVA of Specific wear				
Source	Degrees of Freedom (DOF)	Sum of squares (SS)	Mean Square (MS)	Percentage Contribution
H	3	133.77	44.589	37.59
L	3	173.74	57.914	48.82
S	3	10.17	3.389	2.85
SD	3	21.42	7.139	6.02
Total	15	355.82		100

The coefficient of friction's R-square (percentage of variation) value is 82.13%, which recommends that the model is near to being significant. Table 3 demonstrates the ANOVA for the specific wear with a higher probability percentage of 48.82 for Load, followed by the interaction of heat zone, sliding distance, and speed, with probabilities of 37.59, 6.02, and 2.85, respectively. The R-square (Percentage of variation) value is obtained as 95.30% which displays that the model is significant for specific wear. Additionally, it demonstrates that in the wear behavior of the Al 6101 Aluminium closed cell foam, both the heat zone and the load make significant contributions individually and when combined.

## 4 Conclusion and future recommendations

The objective of this study is to study the wear rate and optimization of wear parameters on Al 6101 closed-cell foam with dissimilar heat and cryogenic treatment zones. Considering Al 6101 foam, this experiment proved that the novel cryogenic treatment has a noteworthy improvement in coefficient of friction and specific wear. Moreover, Taguchi's optimization and ANOVA analysis highlighted that the Al 6101 closed-cell foam specimen in the CHT Zone exhibited optimized results when compared with other heat zones. The following are the conclusions derived from this study.

(1) According to the pin-on-disc wear test graph, it is proved that the CHT specimen exhibited better wear resistance than other heat zone foam specimens. (2) The formation of the oxide layer is higher in the CHT zone foam specimens. It is proved in such a way that the oxide layer in the CHT zone specimen would additionally inhibit the rate of wear. (3) The optimal combination of the coefficient of friction and specific wear, according to the graphic and analytical results of Taguchi's optimization, is a load of 40 N, speed of 400 rpm, and distance of 1500 m for a cryogenic zone and load of 40 N, speed of 400 rpm, and distance of 2000 m for a cryogenic heat zone, respectively. (4) The ANOVA for the specific wear has a higher probability percentage of 48.82 for the load and is followed by the interaction of heat zone, sliding distance, and speed, which have probabilities of 37.59, 6.02, and 2.85, respectively. (5) Taguchi's optimization and ANOVA analysis highlighted that the foam specimen in CHT Zone displayed optimized results when compared with all the other heat zones, the outcomes proved that CHT processing enhanced the wear resistance of the Al 6101 closed-cell foam effectively when compared with various other heat zones.

In the future, the hardness and corrosion resistance properties of the Al 6101 closed-cell foam specimen will be evaluated electrochemically to find the deposition of fine particles on the alloy surface. Furthermore, Taguchi's optimization will be carried out with different speeds, loads, and distances to additionally validate the optimal combinations of the coefficient of friction and specific wear.



**Table 4.** Analysis of Variance: Signal-to-Noise Ratios (S/N), Means for COF, and specific wear

Coefficient of friction (COF)													
Load	3	11.83	11.83	3.944	0.5	0.708	Load	3	0.01692	0.01692	0.005639	0.27	0.847
Speed	3	10.23	10.23	3.41	0.43	0.745	Speed	3	0.02064	0.02064	0.006879	0.33	0.809
Sliding Dis- tance	3	23.02	23.02	7.675	0.97	0.508	Sliding Dis- tance	3	0.05756	0.05756	0.019185	0.91	0.531
Residual Error	3	23.62	23.62	7.873			Residual Error	3	0.0634	0.0634	0.021134		
Total	15	132.16					Total	15	0.3927				
Specific wear													
Signal to Noise Ratios							Means						
Source	DF1	Seq SS2	Adj SS3	Adj MS4	F5	P6	Source	DF1	Seq SS2	Adj SS3	Adj MS4	F5	P6
Heat Zone	3	133.77	133.77	44.589	8	0.061	Heat Zone	3	17.331	17.331	5.777	9.69	0.047
Load	3	173.74	173.74	57.914	10.39	0.043	Load	3	29.69	29.69	9.8968	16.59	0.023
Speed	3	10.17	10.17	3.389	0.61	0.654	Speed	3	2.863	2.863	0.9542	1.6	0.354
Sliding Dis- tance	3	21.42	21.42	7.139	1.28	0.422	Sliding Dis- tance	3	2.423	2.423	0.8078	1.35	0.405
Residual Error	3	16.72	16.72	5.574			Residual Error	3	1.789	1.789	0.5964		
Total	15	355.82					Total	15	54.097				

For Coefficient of friction (COF) -  $S = 2.8059$ ,  $R-Sq = 82.13\%$ ,  $R-Sq (adj) = 10.64\%$  <sup>1</sup>Degrees of freedom, <sup>2</sup>Sequential sums of squares, <sup>3</sup>Adjusted sums of squares, <sup>4</sup>Adjusted mean squares, <sup>5</sup>Statistic ratio, <sup>6</sup>Probability. For Specific wear -  $S = 2.3610$ ,  $R-Sq = 95.30\%$ ,  $R-Sq (adj) = 76.50\%$  <sup>1</sup>Degrees of freedom, <sup>2</sup>Sequential sums of squares, <sup>3</sup>Adjusted sums of squares, <sup>4</sup>Adjusted mean squares, <sup>5</sup>Statistic ratio, <sup>6</sup>Probability.

## References

- Wu G, Xie P, Yang H, Dang K, Xu Y, Sain M, et al. A review of thermoplastic polymer foams for functional applications. *Journal of Materials Science*. 2021;56(20):11579–11604. Available from: <https://doi.org/10.1007/s10853-021-06034-6>.
- Rashid T, Saleem MQ, Mufti NA, Asif N, Ishfaq MK, Naqvi MK. Pressure-Assisted Development and Characterization of Al-Fe Interface for Bimetallic Composite Castings: An Experimental and Statistical Investigation for a Low-Pressure Regime. *Metals*. 2021;11(11):1687. Available from: <https://doi.org/10.3390/met11111687>.
- Krolo J, Lela B, Grgić K, Jozić S. Production of Closed-Cell Foams Out of Aluminum Chip Waste: Mathematical Modeling and Optimization. *Metals*. 2022;12(6):933. Available from: <https://doi.org/10.3390/met12060933>.
- Ubertalli G, Ferraris S. Al-Based Metal Foams (AMF) as Permanent Cores in Casting: State-of-the-Art and Future Perspectives. *Metals*. 2020;10(12):1592. Available from: <https://doi.org/10.3390/met10121592>.
- Zhang W, Xu J. Advanced lightweight materials for Automobiles: A review. *Materials & Design*. 2022;221:110994. Available from: <https://doi.org/10.1016/j.matdes.2022.110994>.
- Zeenath F, Tamilarasan TR, Mohideen S, Milon Selvam D. Mechanical properties and surface characterisation of aluminium foam made of Al 6101 subjected to cryogenic treatment - a comparative study. *International Journal of Materials Engineering Innovation*. 2020;11:244–263. Available from: <https://doi.org/10.1504/ijmatei.2020.108884>.
- Liu M, Li C, Zhang Y, An Q, Yang M, Gao T, et al. Cryogenic minimum quantity lubrication machining: from mechanism to application. *Frontiers of Mechanical Engineering*. 2021;16(4):649–697. Available from: <https://doi.org/10.1007/s11465-021-0654-2>.
- Meng Y, Xu J, Ma L, Jin Z, Prakash B, Ma T, et al. A review of advances in tribology in 2020–2021. *Friction*. 2022;10(10):1443–1595. Available from: <https://doi.org/10.1007/s40544-022-0685-7>.
- Singh P, Pungotra H, Kalsi NS. Parametric optimization of deep cryogenic treatment for the wear response of implant material UNS R56700: Taguchi's approach. *Proceedings of the Institution of Mechanical Engineers, Part H: Journal of Engineering in Medicine*. 2020;234(1):61–73. Available from: <https://doi.org/10.1177/0954411919884775>.
- Prakash U, J, Juliyana J, Saleem S, Moorthy M, V T. Optimisation of dry sliding wear parameters of Aluminium matrix composites (356/B4C) using Taguchi technique. *International Journal of Ambient Energy*. 2021;42(2):140–142. Available from: <https://doi.org/10.1080/01430750.2018.1525590>.
- Sadhana D, A, Prakash U, Ananth J, S, Pillai A, et al. Optimization of wear parameters of Aluminium matrix composites (LM6/Fly Ash) using Taguchi technique. *Materials Today: Proceedings*. 2021;39(4):1543–1548. Available from: <https://doi.org/10.1016/j.matpr.2020.05.550>.
- Sagar SR, Srikanth KM, Jayasimha R. Effect of cryogenic treatment and heat treatment on mechanical and tribological properties of A356 reinforced with SiC. *Materials Today: Proceedings*. 2021;45:184–190. Available from: <https://doi.org/10.1016/j.matpr.2020.10.414>.
- Zhang H, Yan X, Hou Q, Chen Z. Effect of Cyclic Cryogenic Treatment on Wear Resistance, Impact Toughness, and Microstructure of 42CrMo Steel and Its Optimization. *Advances in Materials Science and Engineering*. 2021;2021:1–13. Available from: <https://doi.org/10.1155/2021/8870282>.



- 14) Rahiman AHS, Smart R, S D, Wilson B, Ebrahim I, Eldhose B, et al. Dry sliding wear analysis of Al5083/CNT/Ni/MoB hybrid composite using DOE Taguchi method. *Wear*. 2020;p. 460–461. Available from: <https://doi.org/10.1016/j.wear.2020.203471>.
- 15) Syed ZF, Tamilarasan TR, D MS. Effect of novel cryogenic treatment in the corrosion behaviour, microstructure analysis and electrochemical properties of Al 6101 closed-cell foam. *Australian Journal of Mechanical Engineering*. 2021. Available from: <https://doi.org/10.1080/14484846.2021.1914891>.
- 16) Ali H, Gábora A, Naeem MA, Kalácska G, Mankovits T. Effect of the manufacturing parameters on the pore size and porosity of closed-cell hybrid aluminum foams. *International Review of Applied Sciences and Engineering*. 2021;12(3):230–237. Available from: <https://doi.org/10.1556/1848.2021.00262>.
- 17) Uz D, Solomon MM, Gerengi H, Sahin M, Yıldız M. Shallow cryogenic treatment: effect on the corrosion resistance and hardness properties of AA5083-H111 alloy in chloride-ions enriched medium. *Materials Research Express*. 2021;8(7):076516. Available from: <https://doi.org/10.1088/2053-1591/ac144d>.